Impact of disorder on frequency scaling in the integer quantum Hall effect

K. Saeed,* N. A. Dodoo-Amoo, L. H. Li, S. P. Khanna, E. H. Linfield, A. G. Davies, and J. E. Cunningham
Institute of Microwaves and Photonics, School of Electronic and Electrical Engineering, University of Leeds, Leeds, LS2 9JT, United Kingdom

(Received 4 August 2011; revised manuscript received 7 September 2011; published 31 October 2011)

We have studied the effect of both long- and short-range disorder on frequency scaling of the diagonal magnetoconductivity σ_{xx} in the integer quantum Hall effect regime of two-dimensional electrons confined to $Al_xGa_{1-x}As/Al_{0.33}Ga_{0.67}As$ single heterostructures for two Al concentrations, x. Within the frequency range 100 MHz $\leqslant f \leqslant$ 20 GHz and for a temperature $T = 35$ mK, we found that the frequency scaling exponent c changes from 0.6 ± 0.05 for a $GaAs/Al_{0.33}Ga_{0.67}As$ heterostructure, where the disorder is dominated by long-range ionized impurity potentials, to $c = 0.42 \pm 0.06$ for $Al_{0.015}Ga_{0.985}As/Al_{0.33}Ga_{0.67}As$ heterostructures, where the dominant contribution to the disorder is from short-range alloy potential fluctuations. This value of c allows us to estimate the dynamical scaling exponent as $z = 1 \pm 0.13$.

DOI: 10.1103/PhysRevB.84.155324 PACS number(s): 73.43.Qt, 73.43.Nq

I. INTRODUCTION

In the integer quantum Hall effect,[1,2] two-dimensional electron systems (2DESs) subjected to a perpendicular magnetic field exhibit well-defined transitions between bands of localized and bands of delocalized states. The frequency and temperature scaling behavior of these transitions, accessible through measurements of the conductivity tensor elements σ_{xx} and σ_{xy}, has been an intensely debated topic.[3–5] In general, as the Fermi energy of the system moves from a region of localized to one of delocalized states (a Landau level), the Hall resistance R_{xy} undergoes a sharp increase, whereas the diagonal resistance R_{xx} and diagonal conductivity σ_{xx} first rise and then fall. Within these Landau levels, the electron localization length ξ, which is itself a function of energy E, diverges at some critical energy E_c.[3] For a sample of the finite size L, scaling theory predicts that the components of the conductivity tensor in the transition regions should follow a scaling function of the form $\sigma_{uv}(E) \propto \sigma_{uv}(\frac{L_{\text{eff}}}{\xi})$, with ξ diverging at the critical filling factor ν_c according to $\xi(E) \propto |\nu - \nu_c|^{-\gamma}$, where ν is the filling factor and L_{eff} is the effective sample size.[5] The localization length exponent γ has been predicted to be universal[3,6–8] with a (numerically determined) value of 2.35, which is independent of the material mobility, carrier density, and filling factor. This value was experimentally verified through finite size scaling experiments by Koch *et al.*[9] as well as more recently by Li *et al.*[10] In addition, Polyakov and Shklovskii[11] studied the scaling of the conductivity near ν_c theoretically by considering its dependence on temperature T and frequency f. They showed that the T and f parameters introduce an effective length scale in the scaling function $L_{\text{eff}} = L_T \propto T^{-\frac{p}{2}}$ and $L_{\text{eff}} = L_f \propto f^{\frac{1}{z}}$, respectively, where p is the temperature exponent of the phase coherence length L_ϕ and z is the dynamical scaling exponent. They further demonstrated that as a consequence of these effective length scales, the full width at half maximum ΔB of the σ_{xx} peak should follow a power law $\Delta B(T) \propto T^\kappa$ and $\Delta B(f) \propto f^c$, where κ and c are related to γ through the relations $\kappa = \frac{p}{2\gamma}$ and $c = \frac{1}{z\gamma}$, respectively. κ and c are the critical exponents that can be measured experimentally, allowing for the evaluation of p and z by assuming the theoretical estimate of the critical exponent $\gamma = 2.35$.

To date, the most consistent values of κ measured experimentally have arisen from temperature scaling measurements on InGaAs/InP heterostructures,[12] where the disorder was dominated by short-range alloy potential fluctuations. In Ref. 12, the result $\kappa \approx 0.43$ was found to be independent of sample mobility and filling factor, and it yielded an estimate of $p \approx 2$ for $\gamma = 2.35$. By contrast, measurements on GaAs/AlGaAs heterostructures, where the disorder was dominated by long-range ionized impurity potentials, yielded nonuniversal values for κ ranging from 0.16 to 0.81, dependent on both the sample mobility and the filling factor;[13] in these structures, the screened Coulomb energy has a correlation length on the order of a few micrometers, with an amplitude typically on the order of millielectron volts in the plane of the 2DES.[14] Recently, Al scattering centers have been introduced into the GaAs/AlGaAs materials system to act as a source of short-range potential disorder.[15] It has been shown experimentally[15] that in such $Al_xGa_{1-x}As/Al_{0.33}Ga_{0.67}As$ heterostructures the resulting alloy disorder is short ranged (with a characteristic length scale of the same order as the GaAs lattice constant) and that the scattering potential is strong in amplitude (typically on the order of an electron volt when $0.0065 \leqslant x \leqslant 0.016$). In these structures, κ was found to be $\sim$0.43 for samples where $0.0065 \leqslant x \leqslant 0.016$,[16] similar to that found in InGaAs/InP heterostructures.

The frequency scaling exponent c was first measured in GaAs/AlGaAs systems by Engel *et al.* who found $c \approx 0.43$ within the frequency range 100 MHz $\leqslant f \leqslant$ 15 GHz.[17] The samples measured, however, had a mobility of 40 000 $cm^2V^{-1}s^{-1}$, indicating presence of impurities that may have affected the range of disorder. Hohls *et al.*[18,19] also investigated frequency scaling within the ranges 300 MHz to 6 GHz and 26 GHz to 55 GHz in GaAs/AlGaAs heterostructures using two separate experimental arrangements, finding $c = 0.5 \pm 0.1$. To date, a frequency scaling exponent $c = 0.43$ has not been reported in samples with long-range potential disorder.

In this paper, we report on the effect of both long- and short-range disorder on frequency scaling of the diagonal magnetoconductivity of 2D electrons confined to $Al_xGa_{1-x}As/Al_{0.33}Ga_{0.67}As$ heterostructures, employing a broadband microwave frequency measurement system

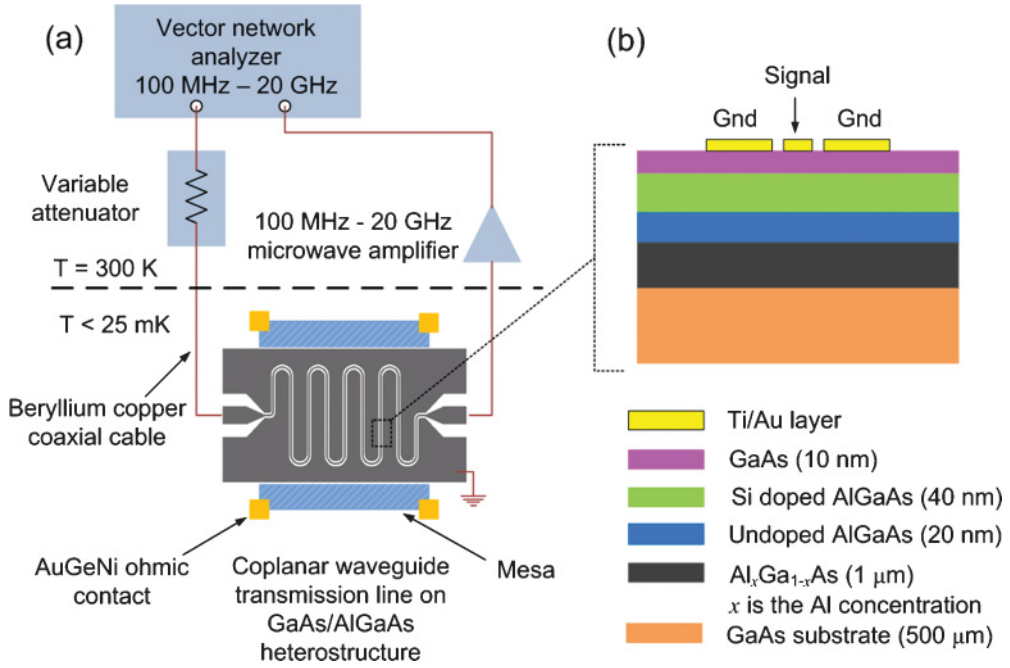

FIG. 1. (Color online) (a) Schematic of experimental setup and (b) Schematic view of the sample structure.

(100 MHz $\leqslant f \leqslant$ 20 GHz). The high-frequency resolution (<70 MHz) of our system allows us to reveal the precise functional form of the conductivity oscillation broadening with frequency, enabling us to obtain accurate estimates of the scaling exponents. We found that in $Al_xGa_{1-x}As/Al_{0.33}Ga_{0.67}As$ heterostructures with $x = 0$, κ depends on both the sample mobility and the filling factor, whereas $c = 0.6$ and is independent of the filling factor. In $Al_xGa_{1-x}As/Al_{0.33}Ga_{0.67}As$ heterostructures with $x = 0.015$, we found $\kappa \approx c \approx 0.43$, independent of the filling factor, thus confirming the universality of κ and c in the short-range disordered regime. Our results highlight the pivotal role played by the nature of the disorder on the values of the critical exponents obtained in frequency scaling experiments. For completeness, we also measured the localization length exponent $\gamma \approx 2.35$ by applying the variable range hopping (VRH) theory deep within the localized regions of the Landau bands to interpret both our temperature- and our frequency-dependent data. The combined measurements of c and γ allow us to estimate the dynamical scaling exponent to be $z \approx 1$.

II. EXPERIMENTAL SETUP

The initial samples used in this work were fabricated from a GaAs-$Al_{0.33}Ga_{0.67}As$ heterostructure grown by molecular beam epitaxy, with unilluminated carrier density $n = 2.89\times10^{11}$ cm^{-2} and direct current (DC) mobility, $\mu = 380\ 000$ cm^{2}V^{-1}s^{-1} at $T = 100$ mK. For $x = 0$, we estimated the background ionized impurity scattering rate $\tau_b^{-1} = e/\mu m^* = 67$ ns^{-1}. In a further set of wafers, small amounts of Al were incorporated into the GaAs during the growth to obtain $Al_xGa_{1-x}As/Al_{0.33}Ga_{0.67}As$ heterostructures, with x determined by careful control of the relative growth rates of Ga and Al. The mobility of these wafers decreased as x was increased. For example, for a nominal value $x = 0.015$, we obtained $\mu = 300\ 000$ cm^{2}V^{-1}s^{-1} and $n = 2.57\times10^{11}$ cm^{-2} at $T = 100$ mK. This suggests a scattering rate $\tau_x^{-1}{}_{=0.015} = 85$ ns^{-1}, which is higher than the background ionized impurity scattering rate. It was shown in Ref. 15 that the scattering rate is independent of T and proportional to $x(1 - x)$ and that for higher Al concentrations (typically $x > 0.02$), a large deviation from this linear dependence is seen, ascribed to correlations between scattering sites because of clustering of Al atoms. For our value of x (0.015), we assumed that the Al scatterers are randomly distributed.

To access the real part of conductivity Re$[\sigma_{xx}(f)]$ at microwave frequencies, we employed a meandered coplanar waveguide (CPW) structure patterned on the top surface of the heterojunction. The CPWs were fabricated using photolithography, and a 20/250-nm Ti/Au layer was deposited on the sample surface by thermal evaporation. A schematic of the sample structure and the experimental arrangement is shown in Fig. 1. A vector network analyzer was used for transmitting and receiving the microwave signal. Coaxial cables were fitted on the insert of a ^{3}He/^{4}He dilution refrigerator (Oxford Instruments Triton DR 200) and were used to couple microwave signals into and out of the CPW of each device. The guided microwave signals coupled strongly with the 2DES in the gap regions (width $w = 30$ μm) between the CPW center conductor and the ground planes. The long lengths of these meandered lines ($l = 20$ mm) ensured a high sensitivity to small changes in the conductivity in magnetic field. DC transport measurements were also made using AuGeNi ohmic contacts to the 2DES arranged in a van der Pauw geometry at the corners of a rectangular mesa beneath the CPW.

The conductivity of the 2DES was related to the power transmitted through the overlaid CPW by modeling the 2DES as a shunt resistance to ground,[20] the total conductance

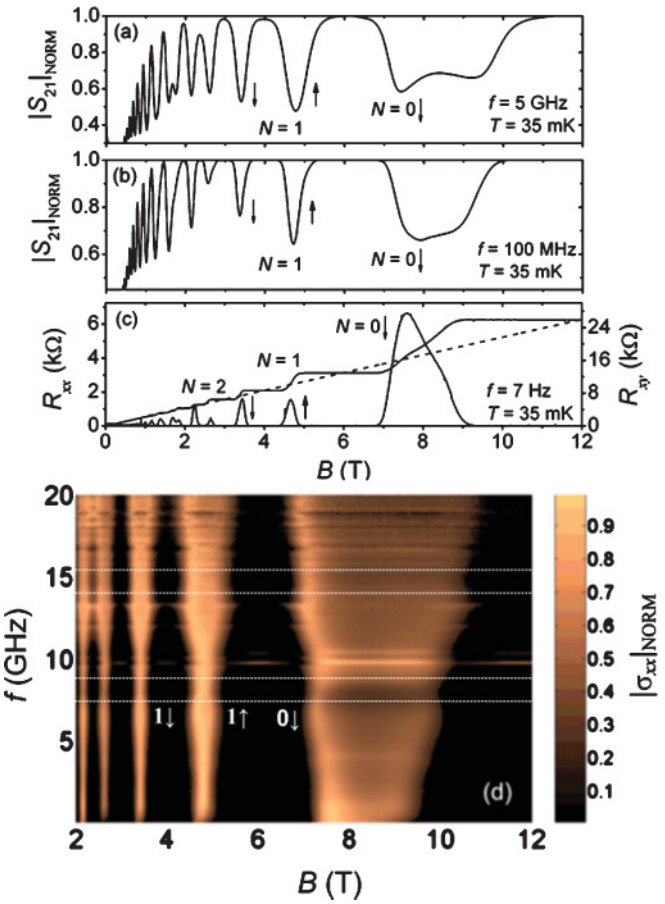

FIG. 2. (Color online) Comparison of normalized transmission $|S_{21}|_{\mathrm{NORM}}$ at (a) $f = 5$ GHz and (b) $f = 100$ MHz. (c) DC Hall (R_{xy}) and longitudinal (R_{xx}) resistances for a $GaAs/Al_{0.32}Ga_{0.67}As$ wafer. The dotted line represents the classical Hall resistance $R_{xy}{}^{o} = B/en$, and N refers to the Landau level index. (d) Contour plot of normalized σ_{xx} vs f and B for $N = 2\downarrow$, $2\uparrow$, $1\downarrow$, $1\uparrow$, and $0\downarrow$ transitions. The dotted-line boxes indicate regions of abrupt narrowing of oscillations. The sample plate temperature was kept at 35 mK, and the input power was $P < 0.01$ nW.

of which is given by $G_T = (2\mathrm{Re}[\sigma_{xx}]l)/w$. The scattering parameter S_{21}, which is the appropriate measure of transmission loss through the device, was then related to $\mathrm{Re}[\sigma_{xx}]$ using $S_{21} = (w + B)/(w + B + (A + Z_o)\mathrm{Re}[\sigma_{xx}]l)$, where $A(f)$ and $B(g,\mathrm{Re}[\sigma_{xx}])$ are correction factors obtained through numerical simulations made using a finite-element electromagnetic field solver; the correction factors were introduced into the equation to take into account variations due to increasing field penetration into the substrate with frequency and the separation g between the 2DES and the CPW. The CPW geometry was chosen such that $Z_o = 50\ \Omega$ to ensure good matching to the coaxial measurement lines.

III. RESULTS AND DISCUSSION

Figure 2(a) and 2(b) shows the magnetic field dependence of S_{21} at frequencies of 100 MHz and 5 GHz, respectively, both at $T = 35$ mK, together with the DC (7 Hz) resistances R_{xx} and R_{xy} (Fig. 2(c)). The S_{21} oscillations correspond to peaks and transitions in R_{xx} and R_{xy}, respectively. For $B >$ 3 T, the zeros in R_{xx} and plateaus in R_{xy} correspond to a flattening of S_{21} at corresponding maximum values of S_{21}, indicating an absence of coupling to the strongly localized 2D electrons at these magnetic fields. The value of the maximum in S_{21} is then determined solely by the losses in the CPW, the CPW–coaxial transition, and the coaxial cables. We use this maximum as a calibration point to subtract out these additional losses, ensuring S_{21} yields values for σ_{xx} that correspond to the 2DES alone. At any given frequency, the constant maximum in S_{21} over the entire magnetic field range indicates that the dominant mode of propagation through the CPW is quasi–transverse electromagnetic, remaining unaffected by the Hall conductivity σ_{xy}. Also noticeable in Fig. 2 is a shoulder that appears on the high-field side of the S_{21} and R_{xx} oscillations for the $N = 0\downarrow$ Landau level index. This shoulder has been ascribed to the presence of attractive impurities in the AlGaAs donor layer.[21,22] Figure 2(d) shows a contour plot of normalized σ_{xx} vs f and B, revealing the precise form of the conductivity oscillation broadening with frequency. An abrupt local narrowing of the oscillations ~8 and 15 GHz can also be seen; numerical simulations indicate the presence of resonant modes within the substrate at these frequencies, which change the electric field distribution on the CPW structure. The resonant modes occur due to the conductive backing of the sample and originate from leakage of microwave energy from one coaxial line to the other through the substrate. The first resonance occurs when the length of the sample is $\approx \frac{\lambda_{\mathrm{eff}}}{2} = \frac{c}{2f\sqrt{\varepsilon_r}}$, where λ_{eff} is the effective wavelength in the GaAs substrate that has a dielectric constant $\varepsilon_r = 12.9$. The second resonance occurs at twice the fundamental resonant frequency. Since the sample length is 5.5 mm, the first and second resonances are expected to occur ~7.5 and 15 GHz, respectively. Data within the range 7.5 GHz $\leqslant f \leqslant$ 8.5 GHz and 14.7 GHz $\leqslant f \leqslant$ 15.2 GHz are therefore excluded from our scaling analysis. We also assessed the extent of electron heating on the 2DES by the applied microwave power P. Using a constant bath temperature of 35 mK, we varied the input power to the CPW while monitoring ΔB for two selected S_{21} oscillations ($N = 1\uparrow$, $1\downarrow$), for different frequencies (Fig. 3). We found that for $P \leqslant 0.1$ nW, ΔB for both transitions remains constant, indicating that the applied microwave power does not cause electron heating. However, for $P > 0.1$ nW, ΔB starts to increase gradually, indicating an increase in the electron temperature. For $P \gg 20$ nW, a significant increase in the sample plate temperature was also observed, resulting from the increased thermal leakage through the coaxial cables. All frequency scaling measurements reported here were carried out with $P < 0.01$ nW.

Figure 4 shows as an example a comparison of the scaling of width ΔB with frequency for two individual oscillations in σ_{xx}, $N = 1\downarrow$ and $N = 1\uparrow$, for both the $GaAs/Al_{0.33}Ga_{0.67}As$ and the $Al_{0.015}Ga_{0.985}As/Al_{0.33}Ga_{0.67}As$ devices. Below 2 GHz, no scaling of the oscillation width is observed with frequency, because the electron heating is predominantly due to the temperature of the sample. Above 2 GHz ($hf \geqslant k_BT$), the oscillation width scales with frequency as $\Delta B \propto f^c$. For the $N = 2\downarrow$, $2\uparrow$, $1\downarrow$, and $1\uparrow$ oscillations, the fits give values of $c = 0.6 \pm 0.05$ and $c = 0.42 \pm 0.06$ within the frequency range 2 GHz $\leqslant f \leqslant$ 20 GHz for the two systems, respectively, independent of the filling factor. The error in c is

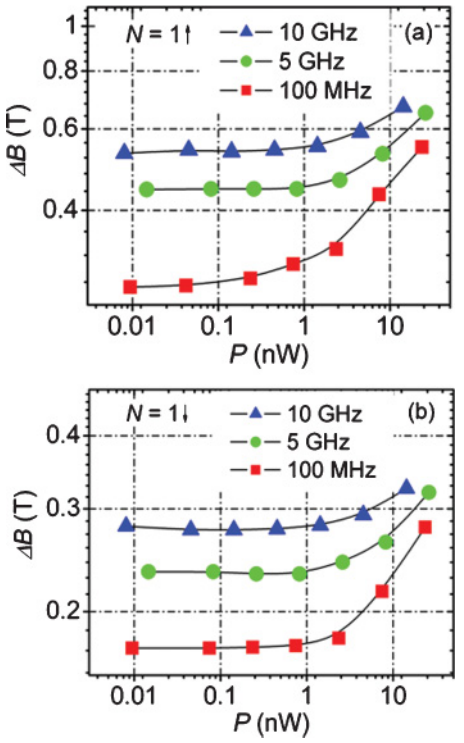

FIG. 3. (Color online) Scaling of the σ_{xx} oscillation width ΔB for (a) $N = 1\uparrow$ and (b) $N = 1\downarrow$ as a function of CPW input power P for three frequencies at a sample plate temperature of 35 mK.

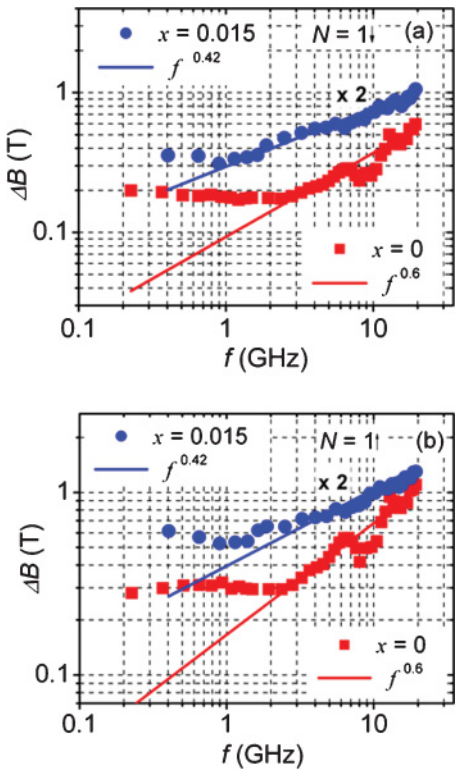

FIG. 4. (Color online) Frequency scaling of σ_{xx} oscillation width ΔB for (a) $N = 1\downarrow$ and (b) $N = 1\uparrow$ transitions for both $Al_{0.015}Ga_{0.985}As$-$Al_{0.33}Ga_{0.67}As$ and $GaAs/Al_{0.33}Ga_{0.67}As$ samples. The solid lines are a fit to the data.

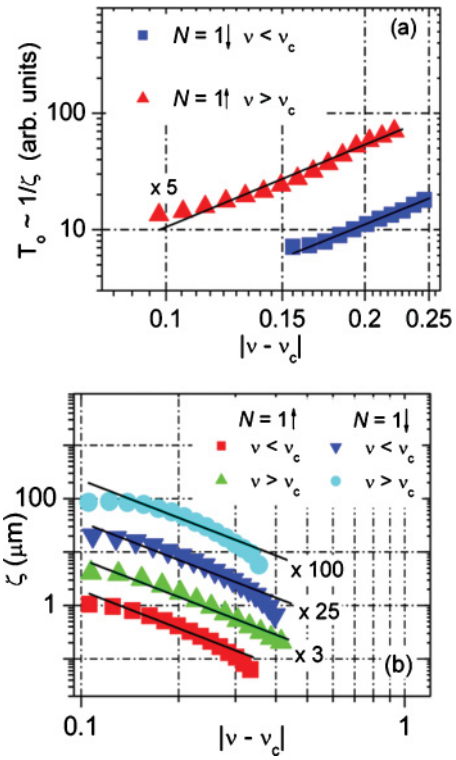

FIG. 5. (Color online) Measured localization length ξ in the Landau band tails with (a) temperature, $\sigma_{xx}(T, f \approx 0)$, and (b) frequency, $\sigma_{xx}(f, T \approx 0)$. The solid black lines in both graphs demonstrate the expected power law behavior $\xi \propto |\nu - \nu_C|^{-\gamma}$ with $\gamma = 2.35$.

estimated from the deviation in the slope of the fitted line over the entire range of fitted frequency points. The value of $c = 0.6$ has also been reported in Ref. 18 for $GaAs/Al_{0.33}Ga_{0.67}As$ heterojunctions.

The different values obtained for c are likely to be a result of the different disorders present in the two heterojunction systems. For the $GaAs/Al_{0.33}Ga_{0.67}As$ samples, the disorder cannot be modeled as an uncorrelated δ-like function potential fluctuation, since its range is comparable to or larger than the length scale of the inelastic scattering length l_{in}.[14] However, for the $Al_{0.015}Ga_{0.985}As/Al_{0.33}Ga_{0.67}As$ samples, the disorder is likely to be dominated by short-range potential fluctuations[15] with a range much less than l_{in}, and universality is restored. The measured values of the exponent c may be used to estimate the dynamical scaling exponent z through the relation $c = 1/z\gamma$, provided that an independent measurement of γ can be performed. For this purpose, measurement of the localization length $\xi \propto |\delta\nu|^{(-\gamma)}$ is required. Following a theoretical proposal in Ref. 11, this can be achieved by measuring σ_{xx} in the tails of the Landau bands, where the electronic conduction is dominated by VRH at low temperatures. From VRH theory, ξ may be calculated either from $\sigma_{xx}(f, T \approx 0)$ in the limit of low temperature or from $\sigma_{xx}(f \approx 0, T)$ in the limit of low frequency via the relations $\mathrm{Re}[\sigma_{xx}(f)] = (\frac{4\pi^2}{3})\varepsilon\varepsilon_o\xi f$ and $\sigma_{xx}(T) \propto \sigma_o \exp[-(\frac{T_o}{T})^{\frac{1}{2}}]$, respectively. Here, $\sigma_o \propto \frac{1}{T}$ and T_o is the hopping temperature, defined as $T_o = \frac{(Ce^2)}{k_B\pi\varepsilon\varepsilon_o\xi}$, where C is a constant. The data measured by Hohls *et al.*[23,25] and

Lewis and Carini[24] was correctly fitted to this predicted frequency dependence. However, the measurements of γ presented in Ref. 24 are for the $N = 0\downarrow$ transition only. As an example, we show corresponding measurements for the $N = 1\uparrow$ and $1\downarrow$ transitions (Fig. 5) calculated using both the frequency and the temperature dependence of σ_{xx} for $Al_{0.015}Ga_{0.985}As/Al_{0.33}Ga_{0.67}As$ samples within the range $0.08 \leqslant |\nu - \nu_c| \leqslant 0.3$. The calculations from VRH theory can only be applied within the tails of the Landau bands. It can be seen that when $|\nu - \nu_c| < 0.15$, we are very close to the region of the delocalized states, and the curve starts to deviate from the predicted dependence shown by the solid lines with the slope 2.35. For $|\nu - \nu_c| > 0.3$, we are close to the zeros of the oscillations, which again results in a deviation from the expected dependence. A convex curving of the graphs similar to the one we obtained was observed in Ref. 23. $\gamma = 2.34 \pm 0.23$ is calculated over the fixed range $0.15 \leqslant |\nu - \nu_c| \leqslant 0.3$. The large error in the value is primarily a result of the extent of curving of the plots for the chosen large range of filling factor. The error is estimated only from the deviation in the slope of the fitted line over the entire range $0.15 \leqslant |\nu - \nu_c| \leqslant 0.3$. The obtained value is in good agreement with that obtained in numerical studies,[3,6–8] thus allowing us to estimate the dynamical scaling exponent $z = 1 \pm 0.13$.

IV. SUMMARY

In conclusion, we studied frequency scaling of the integer quantum Hall effect in 2DESs exhibiting both long- and short-range disorder, using a high-resolution broadband microwave measurement technique. We constructed for the first time a detailed picture showing the precise form of the broadening of the oscillations in diagonal magnetoconductivity with frequency. We found that both temperature and frequency scaling exponents yield nonuniversal values for systems in which disorder is dominated by long-range ionized impurity potentials. However, when the disorder in the system is dominated by short-range alloy potential fluctuations, both exponents yield the same universal values $\kappa \approx c \approx 0.43$. We also separately measured the localization length exponent $\gamma = 2.34 \pm 0.23$ in $Al_{0.015}Ga_{0.985}As/Al_{0.33}Ga_{0.67}As$ wafers by applying VRH theory, allowing us to estimate the dynamical scaling exponent $z = 1 \pm 0.13$.

ACKNOWLEDGMENTS

We acknowledge funding from the Engineering and Physical Sciences Research Council (Reference No. EP/F029543/1), and the Engineering Research Centers program "NOTES". We thank M. Byrne, C. Wood, D. Mistry, and M. Shaukat for valuable discussions.

*k.saeed98@leeds.ac.uk

[1] K. V. Klitzing, G. Dorda, and M. Pepper, Phys. Rev. Lett. **45**, 494 (1980).
[2] A. M. M. Pruisken, in *The Quantum Hall Effect*, edited by R. E. Prange and S. M. Girvin (Springer-Verlag, Berlin, 1986), pp. 117–173.
[3] B. Huckestein, Rev. Mod. Phys. **67**, 357 (1995).
[4] S. L. Sondhi, S. M. Girvin, J. P. Carini, and D. Shahar, Rev. Mod. Phys. **69**, 315 (1997).
[5] A. M. M. Pruisken, Phys. Rev. Lett. **61**, 1297 (1988).
[6] H. Aoki and T. Ando, Phys. Rev. Lett. **54**, 831 (1985).
[7] J. T. Chalker and G. J. Daniell, Phys. Rev. Lett. **61**, 593 (1988).
[8] B. Huckestein and B. Kramer, Phys. Rev. Lett. **64**, 1437 (1990).
[9] S. Koch, R. J. Haug, K. V. Klitzing, and K. Ploog, Phys. Rev. Lett. **67**, 883 (1991).
[10] W. Li, C. L. Vicente, J. S. Xia, W. Pan, D. C. Tsui, L. N. Pfeiffer, and K. W. West, Phys. Rev. Lett. **102**, 216801 (2009).
[11] D. G. Polyakov and B. I. Shklovskii, Phys. Rev. B **48**, 11167 (1993).
[12] H. P. Wei, D. C. Tsui, M. A. Paalanen, and A. M. M. Pruisken, Phys. Rev. Lett. **61**, 1294 (1988).
[13] H. P. Wei, S. Y. Lin, D. C. Tsui, and A.M.M. Pruisken, Phys. Rev. B **45**, 3926 (1992).
[14] J. A. Nixon and J. H. Davies, Phys. Rev. B **41**, 7929 (1990).
[15] W. Li, G. A. Csathy, D. C. Tsui, L. N. Pfeiffer, and K. W. West, Appl. Phys. Lett. **83**, 2832 (2003).
[16] W. Li, G. A. Csathy, D. C. Tsui, L. N. Pfeiffer, and K. W. West, Phys. Rev. Lett. **94**, 206807 (2005).
[17] L. W. Engel, D. Shahar, C. Kurdak, and D. C. Tsui, Phys. Rev. Lett. **71**, 2638 (1993).
[18] F. Hohls, U. Zeitler, R. J. Haug, and K. Pierz, Phys. B **298**, 88 (2001).
[19] F. Hohls, U. Zeitler, R. J. Haug, R. Meisels, K. Dybko, and F. Kuchar, Phys. Rev. Lett. **89**, 276801 (2002).
[20] D. M. Pozar, *Microwave Engineering*, 3rd ed. (John Wiley & Sons, New York, 2004), pp. 49–57.
[21] R. J. Haug, R.R. Gerhardts, K. V. Klitzing, and K. Ploog, Phys. Rev. Lett. **59**, 1349 (1987).
[22] A. Raymond, I. Bisotto, Y. M. Meziani, S. Bonifacie, C. Chaubet, A. Cavanna, and J. C. Harmand, Phys. Rev. B **80**, 195316 (2009).
[23] F. Hohls, U. Zeitler, R. J. Haug, R. Meisels, K. Dybko, and F. Kuchar, Phys. E **16**, 10 (2003).
[24] R. M. Lewis and J. P. Carini, Phys. Rev. B **64**, 073310 (2001).
[25] F. Hohls, U. Zeitler, and R. J. Haug, Phys. Rev. Lett. **88**, 036802 (2002).